Tetrahedron 64 (2008) 5370–5378

Contents lists available at ScienceDirect

Tetrahedron

journal homepage: www.elsevier.com/locate/tet

p-Sulfonatocalix[7]arene: synthesis, protolysis, and binding ability

Carmine Gaeta, Tonino Caruso, Milena Mincolelli, Francesco Troisi, Ermanno Vasca *, Placido Neri *

Dipartimento di Chimica, Università di Salerno, Via Ponte don Melillo, I-84084 Fisciano, Salerno, Italy

ARTICLE INFO

Article history:
Received 22 November 2007
Received in revised form 12 February 2008
Accepted 6 March 2008
Available online 18 March 2008

Keywords:
Calixarenes
Calix[7]arenes
Water-soluble
Molecular recognition
pK_a
Spectrofluorimetry

ABSTRACT

Water-soluble *p*-sulfonatocalix[7]arene **1** has been synthesized in good yield through standard procedures and its conformational preferences have been investigated by Monte Carlo conformational searches. The acid–base properties of **1** were investigated by means of potentiometric titration, obtaining pK_a values in agreement with those reported for other *p*-sulfonatocalix[*n*]arene homologs. The binding ability of **1** toward organic quaternary ammonium cations such as Diquat (**2**), Paraquat (**3**), and Chlormequat (**4**) was investigated by means of ^{1}H NMR titrations in D_2O at pD=7.3, DOSY NMR measurements, and 2D ROESY NMR spectroscopy. Spectrofluorimetry proved to be a useful method for the determination of trace amounts of **2** and **3** in aqueous solution by using Acridine Orange bound to **1** as a chemical indicator.

1. Introduction

Molecular recognition[1] is an intensely active current area of research, the main aim of which is the preparation of new functional material with potential applications as sensors,[2] chromatographic stationary phases for separation processes,[3] and membranes and extractants for pollutants removal.[4] Among the more effective synthetic supramolecular receptors, calixarene[5] hosts are of special interest. They are bowl-shaped macrocycles endowed with a cavity able to host small molecules or ions. A wide variety of functional groups may be introduced onto the macrocycle, either at the upper (or wider) and at the lower (or smaller) rim. Special attention has been devoted to the recognition properties of calixarene derivatives in water, because it is the solvent of biological reactions. The scarce solubility of native calixarene macrocycles in aqueous solutions may be suitably enhanced by introducing sulfonato groups at their upper rim.[6] This allowed an investigation of the binding ability of the so-called 'major' *p*-sulfonatocalix[*n*]arenes (those in which *n*=4, 6, and 8)[6] toward amino acids and nucleic acid bases,[7] peptides,[8] organic ammonium cations,[9] neutral guests,[10] and other biologically interesting molecules such as steroids[11] (testosterone, progesterone, estradiol) and neurotransmitter (acetylcholine).[12] In particular, the recognition properties of *p*-sulfonatocalix[4]arene toward organic ammonium cations have been investigated by microcalorimetry and NMR, indicating that the electrostatic interactions between sulfonato and ammonium groups are fundamental for adduct stability.[13] Recently, Liu et al. have reported a study on the recognition of 4,4′-dipyridine, 2,2′-dipyridine, and 1,10-phenanthroline by *p*-sulfonatocalix[5]arene and *p*-sulfonatocalix[4]arene at various pH.[14] Their data indicate that the binding of these guests is favored by the enthalpic contribution, indicating that the stabilization of the host–guest adduct is determined by secondary forces (H-bonds, CH···π, π···π, and electrostatic interactions).[14] The size of the calixarene cavity also plays a pivotal role in the binding process.[7f] Thus, in the above reported case, both 2,2′-dipyridine and 1,10-phenanthroline showed a higher association constant for *p*-sulfonatocalix[4]arene than *p*-sulfonatocalix[5]arene, whereas the situation is reversed in the case of 4,4′-dipyridine. Besides, recently Arena et al.[7f] have observed that the inclusion of amino acids in *p*-sulfonatocalix[4]arene derivatives depends on the cavity dimension: *p*-sulfonatocalix[4]arene derivative in a C_{2v} conformation has a narrow cavity, in which there is not enough space to accommodate amino acids. Differently from the major even-homologs, the synthesis and the recognition properties of *p*-sulfonatocalix[7]arene have not yet been reported. On the other hand, the recognition properties of calix[7]arene[15] derivatives can be of significant interest because of the different dimension of the macrocyclic cavity and of the peculiar conformational properties of this new host.[16,17] These intriguing aspects prompted us to investigate the synthesis and the recognition properties of *p*-sulfonatocalix[7]arene (**1**) toward some organic quaternary ammonium ions of environmental relevance, namely Diquat (*1,1′-ethylene-2,2′-bipyridinium*, **2**) dibromide, Paraquat (*1,1′-dimethyl-4,4′-bipyridinium*, **3**) dichloride and Chlormequat (*2-chloroethyltrimethylammonium*, **4**)

* Corresponding authors. Tel.: +39 089969572; fax: +39 089969603 (P.N.); tel.: +39 089969588; fax: +39 089969603 (E.V.).
E-mail addresses: evasca@unisa.it (E. Vasca), neri@unisa.it (P. Neri).

0040-4020/$ – see front matter © 2008 Elsevier Ltd. All rights reserved.
doi:10.1016/j.tet.2008.03.017

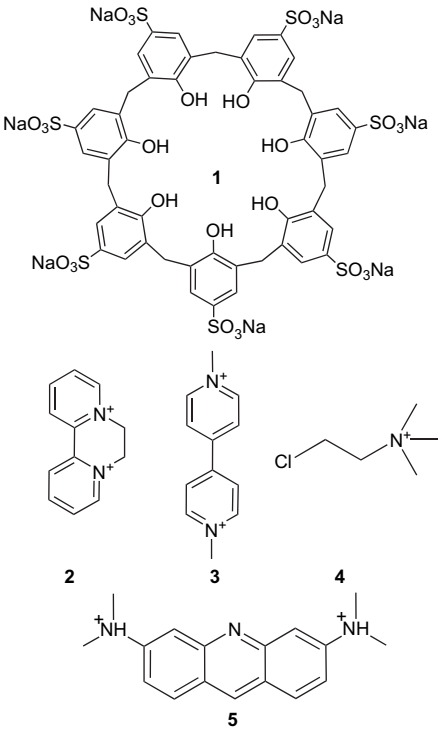

chloride, by means of NMR spectroscopy and spectrofluorimetry. Herein, we wish to report the results of these studies.

2. Results and discussion

The synthesis of *p*-sulfonatocalix[7]arene **1** followed a classical procedure starting with *p*-*tert*-butylcalix[7]arene, which was synthesized under Gutsche's acidic conditions.[18] *p*-*tert*-Butylcalix[7]arene was de-*tert*-butylated with $AlCl_3$ in toluene following the reported procedure,[19] and successively treated with 96% H_2SO_4 for 3 h at 80 °C. After a workup procedure based on the addition of $Ba(OH)_2/Na_2CO_3$ and very similar to that reported by Shinkai,[6b] we have obtained the nonasodium salt of calix[7]arene-*p*-heptasulfonate **1** as a white precipitate.[26] The ^1H NMR spectrum in D_2O (400 MHz, 25 °C) of **1**, showed two sharp singlets relative to $ArCH_2Ar$ and ArH protons, indicating a high conformational mobility of the macrocycle. The presence of two signals in the ^1H NMR spectrum of **1** was consistent with a calix[7]arene structure possessing a C_{7v} molecular symmetry. A better insight into the conformation of the *p*-sulfonatocalix[7]arene **1** was obtained by Monte Carlo conformational searches using the MacroModel-9.0 program[20] [OPLS (Optimized Potentials for Liquid Simulations) force field, H_2O solvent]. The starting structures were built on the basis of the most common conformations adopted by calix[7]arene skeleton as found in the X-ray crystal structures.[16,21] On the basis of the elemental analysis and of the pK_a values reported in the following section, *p*-sulfonatocalix[7]arene possesses two readily ionizable phenolic protons, and at neutral pH exists as the [*p*-sulfonatocalix[7]arene]$^{9-}$ anion. In accordance with these considerations, location of the phenoxide anions at the 1,4 positions always led to a lower energy with respect to all the other ones. Therefore, all conformational searches were conducted on this dianion. The lowest OPLS-energy conformation found by these means and depicted in Figure 1a is consistent with the X-ray structure[16] and lowest MM3-energy conformation found by Harada and Shinkai[17] for native calix[7]arene skeleton and defined as double-cone pinched. Instead, *p*-sulfonatocalix[7]arene built on the basis of the X-ray pleated-loop/cone structure (Fig. 1b) reported by Perrin et al. for *p*-ethylcalix[7]arene,[21a] shows an energy higher by 7.0 kJ/mol than that of the double-cone pinched, in accordance with the energy considerations reported by Harada and Shinkai[17] on calix[7]arene macrocycle. Other common X-ray conformations of the calix[7]arene skeleton were found at consistently higher energies. In the double-cone pinched conformation of *p*-sulfonatocalix[7]arene **1** both phenoxide anions at the lower rim are hydrogen bonded to their

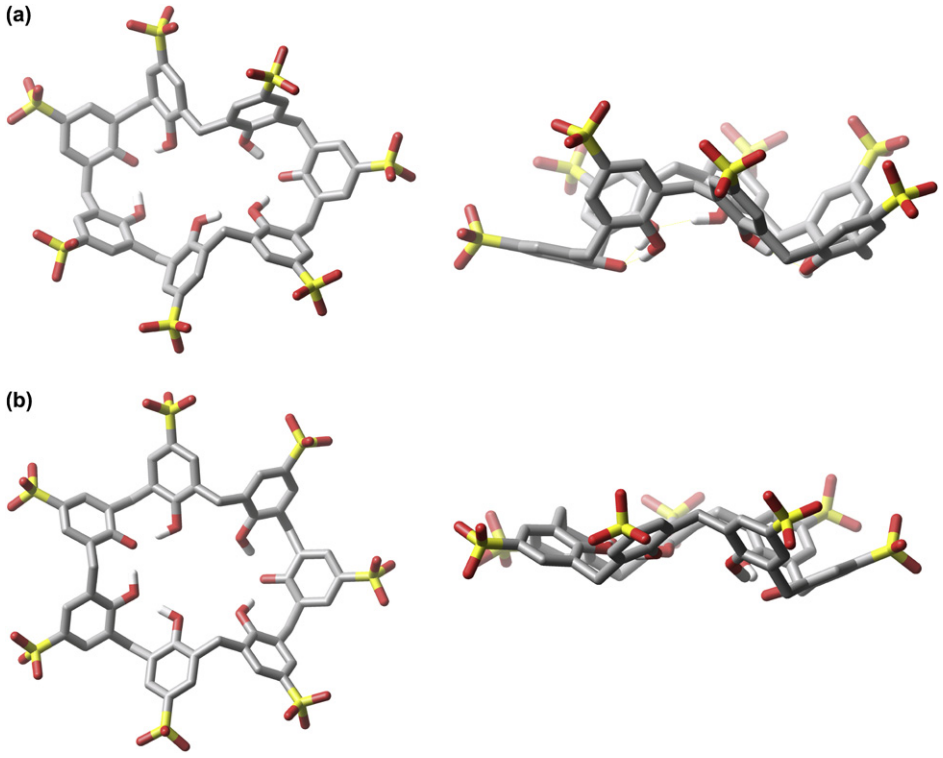

Figure 1. Lowest OPLS-energy structures of the *double-cone pinched* (a) and *pleated-loop/cone* (b) conformations of *p*-sulfonatocalix[7]arene **1**.

flanking OH groups as shown in Figure 1a. Analogous stabilization occurs for the two phenoxide anions of pleated-loop/cone conformation (Fig. 1b).

2.1. Potentiometric determination of the acid dissociation constants of *p*-sulfonatocalix[7]arene

The acid–base properties of **1** in water were investigated potentiometrically, at 25 °C. Considering that in aqueous solution the Na^+ ions balancing the sulfonato residues of **1** are 100% dissociated, a high charge for **1** was expected. As a consequence, the ionic strength of the solution varies with pH and variations of activity coefficients of the reacting species occur, which lead to inaccurate equilibrium constants. As may be easily demonstrated by using the Specific Interaction Theory,[22] an effective control of the activity coefficient variations of **1** could be obtained by adding to the solution under investigation a thousand fold excess of a 100% dissociated electrolyte. Thus, all the solutions were prepared so as to contain 3 M $NaClO_4$ as the ionic medium. Experiments were performed in the form of potentiometric titrations in which constant-current coulometry was used to vary the pH of the solutions. The analytical acidity, H_0, of an accurately known volume, V_0, of a *p*-sulfonatocalix[7]arene (in the following Na_7H_7L) solution

$$\mathrm{S}: \mathrm{Na_7H_7L}\ C_0\ \mathrm{M}, \mathrm{HClO_4}\ H_0\ \mathrm{M}, \mathrm{NaClO_4}(3.000 - H_0)\ \mathrm{M}$$

in which $C_0 \cong 10^{-3}$ M, high enough to suppress the dissociation of the hydroxyl protons, was decreased stepwise by using the circuit I

$$(-)\mathrm{Pt}\,|\,\mathrm{Solution\ S}\,|\,\mathrm{AE}(+) \quad \text{(I)}$$

in which a platinum foil (1 cm^2 area) was the cathode and

$$\mathrm{AE}: \mathrm{NaClO_4}\ 3.000\ \mathrm{M}\,|\,\mathrm{NaClO_4}\ 2.980\ \mathrm{M}, \mathrm{HClO_4}\ 0.010\ \mathrm{M}, \mathrm{Hg_2(ClO_4)_2}\ 0.050\ \mathrm{M}, \mathrm{Hg}$$

was the anode, an auxiliary electrode electrically connected with S through a salt bridge. The stepwise delivery of an accurately known current intensity into S for a pre-fixed time interval allowed the determination of the micromoles of H^+ ions reduced at each step at the cathode of (I), μ. After each addition, the electromotive force E was measured (in the following emf), at the ends of the galvanic cell (II)

$$\mathrm{RE}\,|\,\mathrm{Solution\ S}\,|\,\mathrm{GE} \quad \text{(II)}$$

In cell (II)

$$\mathrm{RE}: \mathrm{Ag, AgCl}\,|\,\mathrm{AgClO_4}\ 0.010\ \mathrm{M}, \mathrm{NaClO_4}\ 2.990\ \mathrm{M}, \mathrm{AgCl_{(s)}\,satd}\,|\,\mathrm{NaClO_4}\ 3.000\ \mathrm{M}$$

was a reference Ag, AgCl electrode (RE), external to the cell but in electrical contact with it through a salt bridge, and GE was a glass membrane electrode. As a criterion for the attainment of a true equilibrium an emf value varying by less than ±0.01 mV over 15 min was assumed. In order to verify both the reversibility of the equilibria and that no electrochemical reduction of **1** had occurred at the cathode, once a 10^{-3} mol/dm^3 excess of hydroxide ions had been produced, the polarity of cell (I) was reversed, and a back titration was performed. The primary $(\mu, E)_{C0}$ data thus collected were used to determine the equilibrium constants, K_n, of the reaction 1

$$\mathrm{H_7L^{7-}} + n\mathrm{H_2O} \rightleftarrows n\mathrm{H_3O^+} + \mathrm{H_{(7-n)}L^{(7+n)-}} \quad (1)$$

Obviously the actual charge of the species was different from the formal one appearing in Eq. 1, owing to the variable amount of Na^+ ions partially neutralizing **1**; however, because of the use of the constant ionic medium method it was not possible to determine the true number of Na^+ and/or ClO_4^- ions appearing in each species, because their concentration was not varied during the experiments.

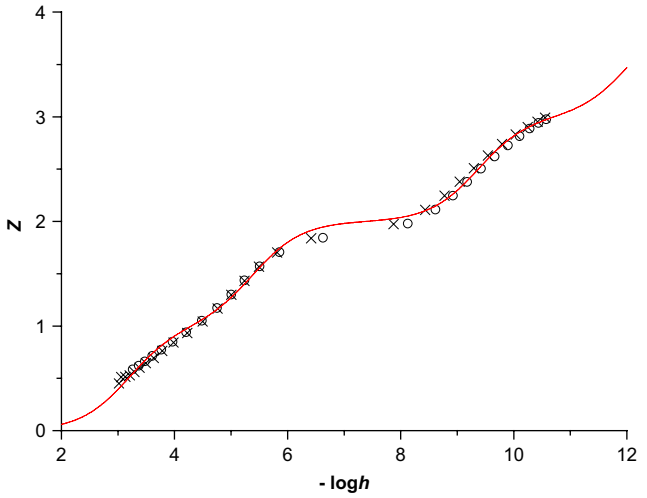

Figure 2. Plot of the primary data of the potentiometric titration of **1** as the formation function Z versus $-\log h$, for the direct (circles) and the back (crosses) titration. The solid curve was obtained from Eq. 4, assuming $\log K_1 = -3.19$; $\log K_2 = -8.59$; $\log K_3 = -18.0$; $\log K_4 = -30.0$.

In order to evaluate K_n, both H, the analytical proton excess with respect to the zero level represented by H_7L^{7-} and H_2O, and the concentration of H_3O^+ ions at equilibrium, h ($\equiv[H_3O^+]$), had to be determined; the first on the basis of Eq. 2

$$H = (H_0V_0 - \mu)/V_0 \quad (2)$$

and the second from the Nernst equation for cell (I) at 25 °C.

$$E = E^0 + 59.16 \log h \quad (3)$$

The constant terms H_0 in Eq. 2 and E^0 in Eq. 3 were determined, simultaneously, in a preliminary stage of each experiment with the Gran's method.[23] The (h, H) data were the basis for the evaluation of the formation function

$$Z = (h - H)/C_0 = \left(\sum nK_n h^{-n}\right) \Big/ \left(1 + \sum K_n h^{-n}\right) \quad (4)$$

representing the average number of H^+ ions dissociated per each *p*-sulfonatocalix[7]arene. A plot of the $Z(-\log h)$ data collected is presented in Figure 2. As it is evident from an inspection of Figure 2, a full reversibility of the protolytic equilibria occurs. The equilibrium constants K_n were evaluated from a least-squares regression of the $Z(-\log h)$ points. The best fit was obtained with the following set of values: $\log K_1 = -3.19 \pm 0.06$; $\log K_2 = -8.59 \pm 0.09$; $\log K_3 = -18.0 \pm 0.1$; $\log K_4 = -30.0 \pm 0.8$ (the uncertainties representing three times the standard deviation), corresponding to the following stepwise dissociation constants: $pK_{a1} = 3.19$; $pK_{a2} = 5.40$, $pK_{a3} = 9.41$, $pK_{a4} = 12.0$, in accord with pK_a values reported for analogous *p*-sulfonatocalix[*n*]arenes ($n = 5$ and 6).[24] The distribution diagram of **1** in the 10^{-2}–10^{-12} M acidity interval is presented in Figure 3. Perusal of the pK_{an} suggests that the dissociation of the first hydroxyl proton is favored by the formation of strong hydrogen bonds within the lower rim, as in Figure 4a. A similar stabilization of the dianion formed after a further proton dissociation is expected, on the basis of a hydrogen bond network as the one depicted in Figure 4b.

2.2. NMR determination of the binding ability of *p*-sulfonatocalix[7]arene toward Diquat, Paraquat, and Chlormequat

The recognition properties of *p*-sulfonatocalix[7]arene (**1**) toward some organic quaternary ammonium ions of environmental

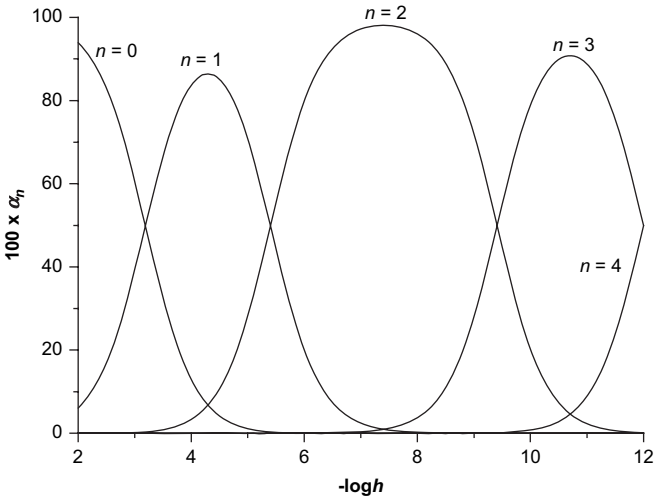

Figure 3. Distribution diagram of the $H_{(7-n)}L^{(7+n)-}$ species at 25 °C in the $2 \leq -\log h \leq 12$ interval. α_n represents the concentration of the $H_{(7-n)}L^{(7+n)-}$ species relative to the total concentration of **1**. The plot was drawn assuming the constants $\log K_1 = -3.19$; $\log K_2 = -8.59$; $\log K_3 = -18.0$; $\log K_4 = -30.0$, determined in 3 M $NaClO_4$.

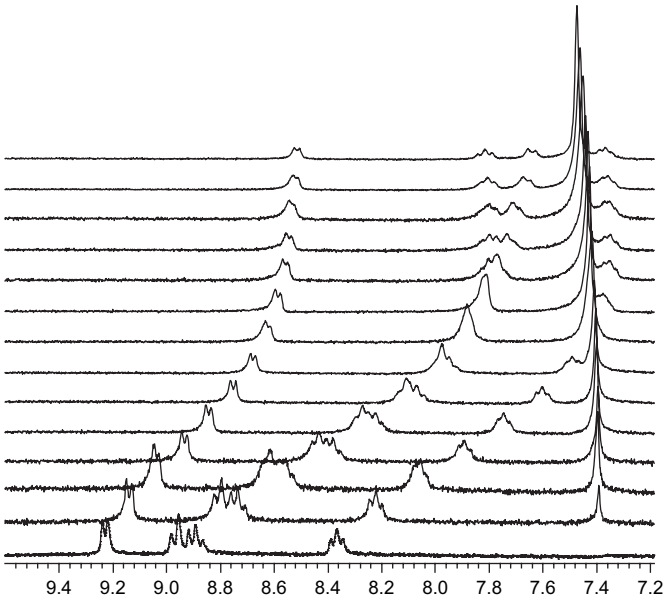

Figure 5. Titration of Diquat **2** with *p*-sulfonatocalix[7]arene **1**. Aromatic region of the ^1H NMR spectrum (400 MHz, 25 °C, 0.1 M phosphate buffer in D_2O) of Diquat **2** after addition of (from bottom to top) 0.00, 0.11, 0.23, 0.35, 0.46, 0.57, 0.68, 0.80, 0.91, 1.00, 1.12, 1.23, 1.43, and 1.64 equiv of **1**.

relevance, namely Diquat (*1,1′-ethylene-2,2′-bipyridinium*, **2**) dibromide, Paraquat (*1,1′-dimethyl-4,4′-bipyridinium*, **3**) dichloride, and Chlormequat (*2-chloroethyltrimethylammonium*, **4**) chloride, were investigated by means of NMR titrations.[25]

^1H NMR titrations were carried out by increasing the [host]/[guest] ratio, while keeping constant, at about 10^{-3} mol/dm^3, the guest concentration. In all cases the signals of guest protons were observed as averaged single resonances because of the fast exchange on the NMR timescale between the free and bonded guest.[26]

The chemical shift of the guest protons usually shifted to higher fields upon addition of the host (Fig. 5).[26]

The observed upfield shifts are very likely determined by shielding effects of the aromatic nuclei consequent to the penetration of the guest into the cavity of the host. In all cases the stoichiometry for the reaction 5 is 1:1 as was confirmed by Job plots[25,26] (Fig. 6, insets) (in which **G** may be **2**, **3** or **4**).

$$\mathbf{1} + \mathbf{G} \rightleftarrows \mathbf{1}\cdot\mathbf{G} \quad (5)$$

Figures 5 and 6a show the changes in the chemical shift ($\Delta\delta_{obs} = \delta_{obs} - \delta_{free}$) induced by inclusion of Diquat (**2**) into the cavity of *p*-sulfonatocalix[7]arene (**1**). As reported,[13c,14,27] these values are useful to obtain information about the structure of the complexes. As shown in Figure 6a, for Diquat (**2**) the higher CIS (Complexation Induced Shift) was observed for protons H(d), while the lowest CIS was experienced by the ethylene bridge protons and by the H(a) protons. The $\Delta\delta$ value are consistent with the binding mode described in Figure 7, in which the guest **2** is sandwiched within the calixarene aromatic walls, with positive nitrogen atoms close to anionic sulfonato groups to maximize the electrostatic interactions. This is substantially in agreement with the binding mode proposed by Liu et al.[14] for the inclusion of the protonated 2,2′-dipyridine into the cavity of *p*-sulfonatocalix[5]arene.

The binding mode of the complex **1**·**2** depicted in Figure 7, was confirmed by a 2D ROESY spectrum (see Fig. S7 in Supplementary data). In fact, a weak cross-peak at 8.54/7.46 ppm between H(a) proton of Diquat **2** and aromatic Ar–H protons of *p*-sulfonatocalix[7]arne **1** can be seen in the ROESY spectrum of the complex **1**·**2**. In addition, a strong cross-peak was present at 7.82/7.46 ppm between the broad singlet relative to H(b) and H(d) proton of **2** and Ar–H protons of *p*-sulfonatocalix[7]arne **1**, indicating their closer spatial proximity.

Recently, Diffusion-Ordered SpectroscopY (DOSY) NMR has been particularly used in host–guest chemistry[9a,28] to rule out the possibility of 2:2 complexes in the form of a molecular capsule,[29] or other higher order species. Thus, we decided to perform DOSY NMR measurements to investigate these aspects for the complex

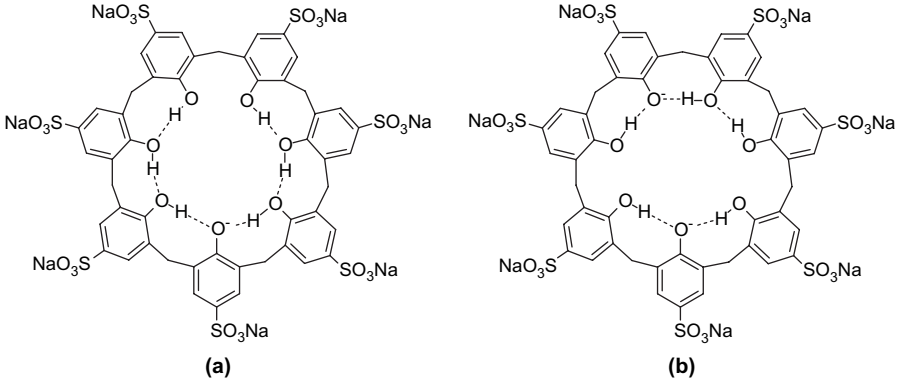

Figure 4. Stabilizing hydrogen bonds in H_6L^{8-} (a) and H_5L^{9-} (b) anions.

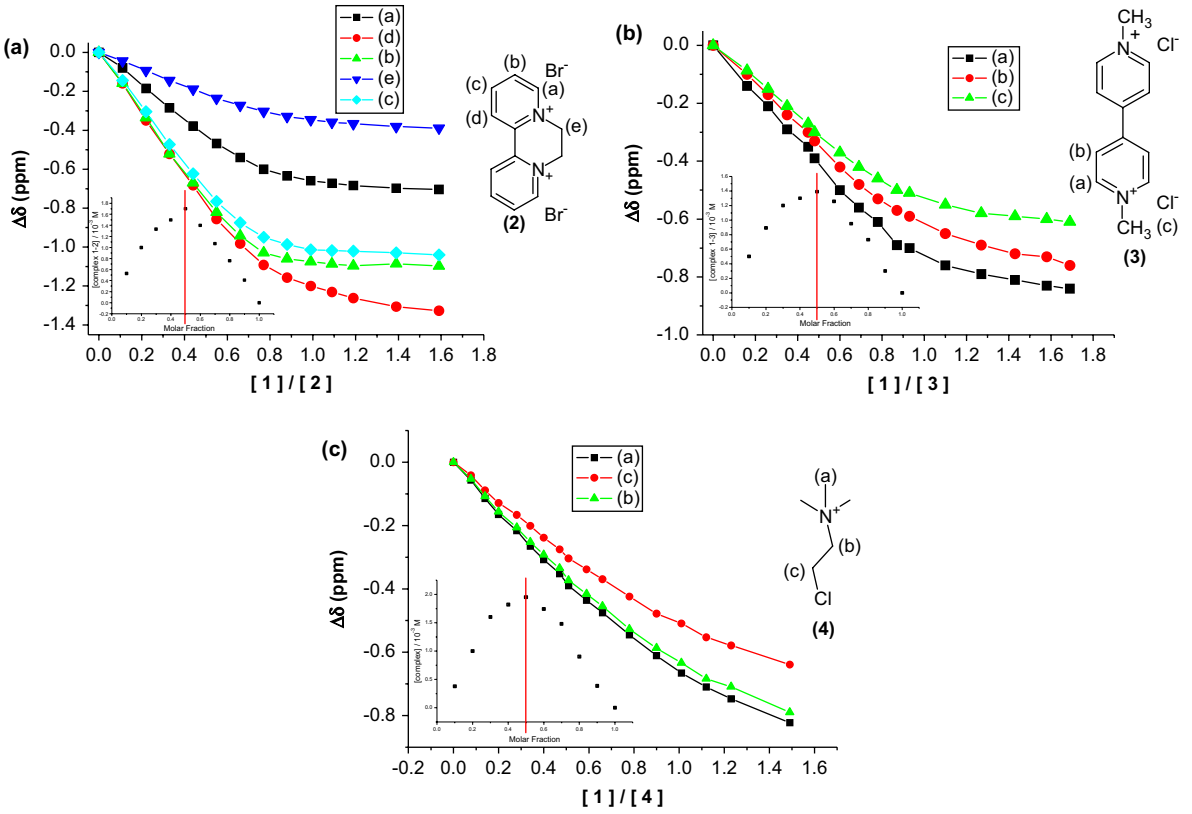

Figure 6. Plots of the $\Delta\delta$ (ppm) of the protons of Diquat **2** (a), Paraquat **3** (b), and Chlormequat **4** (c) versus [*p*-sulfonatocalix[7]arene]/[*n*] (*n*=**2**, **3**, and **4**), at 25 °C in D_2O (400 MHz) and 0.1 M phosphate buffer (pD=7.3.). [**2**]=1.4 mM, [**3**]=1.8 mM, [**4**]=1.8 mM. Insets: Job's plots.

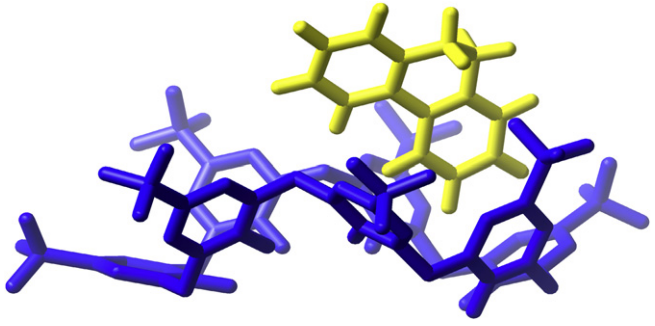

Figure 7. Energy-minimized structure of the complex formed between *p*-sulfonatocalix[7]arene **1** (blue) and Diquat **2** (yellow) (MacroModel V. 9.0, OPLS force field).

formed between *p*-sulfonatocalix[7]arene **1** and Diquat **2** (Fig. 8). In particular, in a phosphate buffer at 298 K, we obtained a diffusion coefficient of 6.14×10^{-10} m^2/s for Diquat **2** (Table 1), while in a 1:1 mixture with *p*-sulfonatocalix[7]arene **1** Diquat **2** showed a significant decrease in the diffusion rate (3.37×10^{-10} m^2/s). This indicates that *p*-sulfonatocalix[7]arene **1** and Diquat **2** form a stable complex, which diffuses more slowly than free Diquat **2**. The DOSY technique, in addition, provides information about the size of the molecular aggregate in solution. In fact, by means of the Stokes–Einstein equation, the diffusion coefficient of the complex **1**·**2** can be converted into its hydrodynamic radius R_h and this value can be compared with the calculated radius obtained by OPLS-minimized structure of the complex **1**·**2** (Fig. 7). Thus, combining the diffusion coefficient of the complex **1**·**2** ($D=3.37\times10^{-10}$ m^2/s) with the viscosity of D_2O[30] at 298 K in the Stokes–Einstein equation ($R=k_BT/6\pi\eta D$; where k_B is the Boltzmann constant, T is the absolute temperature, and η is the viscosity of D_2O at 298 K),[30] a hydrodynamic radius $R_{h(exp)}$=7.28 Å was obtained. This value is in good agreement with the hydrolytic radius $R_{h(calcd)}$=8.70 Å calculated from the OPLS-minimized structure of the complex **1**·**2** shown in Figure 7. In conclusion, the results of DOSY experiments are in accord with the 1:1 stoichiometry deduced by means of Job's plot. In fact, the calculated hydrodynamic radius (7.28 Å) matched very well with the theoretical value of the 1:1 complex for **1**·**2** (8.70 Å), ruling out the possibility of higher order host–guest complexes, such as molecular capsules of the type reported by Dalgarno et al.[29]

In the case of Paraquat **3**, upon complexation with *p*-sulfonatocalix[7]arene (Fig. 6b) higher CIS were observed for H(a) and H(b) aromatic protons with respect to methyl groups.[26] The inclusion of the Paraquat **3** into the cavity of *p*-sulfonatocalix[7]arene **1** was confirmed by a 2D ROESY spectrum (see Fig. S8 in Supplementary data). In fact, this spectrum exhibits cross-peaks at 8.31/7.51 ppm between H(a) proton of Paraquat **3** and aromatic Ar–H protons of *p*-sulfonatocalix[7]arene **1**, and cross-peaks at 7.71/7.51 ppm between the singlet relative to H(b) and Ar–H protons of *p*-sulfonatocalix[7]arene **1**.[26] In addition, a cross-peak between methyl groups of Paraquat **3** and aromatic ArH protons of the *p*-sulfonatocalix[7]-arene **1** at 3.90/7.51 was indicative of the inclusion of the Paraquat **3** into the cavity of *p*-sulfonatocalix[7]arene **1**.[26] DOSY NMR data (Fig. 9) were consistent with a 1:1 stoichiometry of the complex **1**·**3** as determined by means of Job's plot. In fact, the hydrodynamic radius of the complex **1**·**3** $R_{h(exp)}$=8.72 Å (Table 1) derived by diffusion rate ($D=2.32\times10^{-10}$ m^2/s) was in good agreement with hydrolytic radius of the complex **1**·**3**, $R_{h(calcd)}$=8.83 Å (Table 1) calculated from the OPLS-minimized structure of the complex **1**·**3**.[26]

In the case of Chlormequat 4 (Fig. 6c) a higher complexation induced shift was observed for ammonium methyl protons,

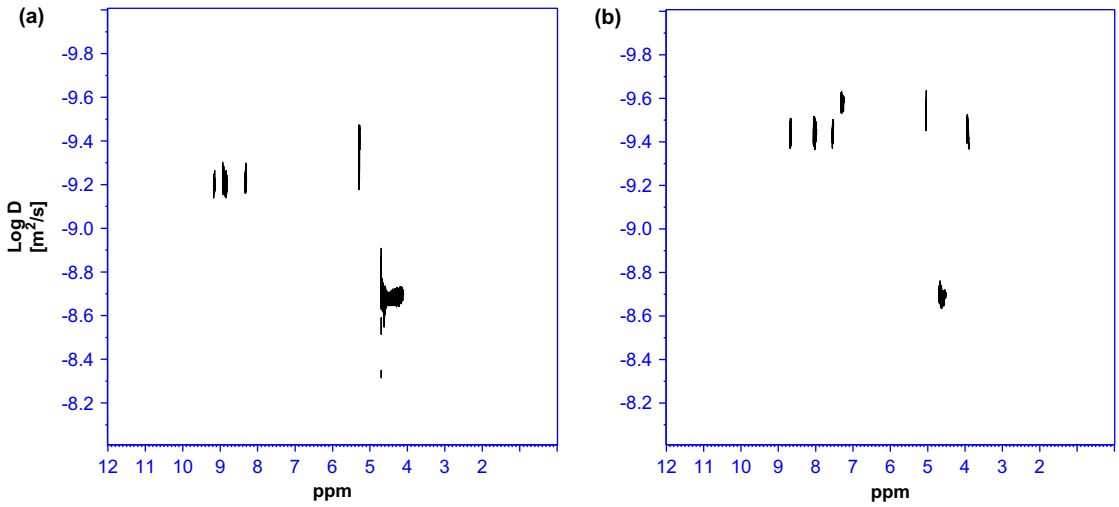

Figure 8. 2D-DOSY spectra recorded in 0.1 M deuterated phosphate buffer, pD 7.3 at 300 K with: (a) Diquat **2** and (b) mixture of *p*-sulfonatocalix[7]arene **1** and **2** in a 1:1 ratio.

Table 1
Diffusion coefficients and experimental $R_{h(exp)}$ and calculated $R_{h(calcd)}$ hydrolytic radii for the complexes **1**·**2** and **1**·**3**

	$D^a/10^{-10}$ m²/s	$R_{h(exp)}{}^b$/Å	$R_{h(calcd)}{}^b$/Å
Diquat **2**	6.14		
Complex **1**·**2**	3.37	7.28	8.70
Paraquat **3**	8.00		
Complex **1**·**3**	2.32	8.72	8.83

[a] The NMR diffusion measurements were performed on 5 mM samples in 0.1 M deuterated phosphate buffer, pD 7.3 at 300 K.

[b] The experimental hydrodynamic radii were calculated by means of the Stokes–Einstein equation (assuming spherical shape of all the assemblies) using the corresponding diffusion coefficients. These values were compared with the average radius ($R_{h(calcd)}$, see table) of the energy-minimized structures of the complexes obtained by means Monte Carlo conformational searches (50,000 steps, MacroModel OPLS force filed).

consistently with the inclusion of this charged group into the cavity to give C–H···π interactions.[26]

The association constants $K_{\mathbf{1}\cdot\mathbf{G}}$ of the three complexes were determined either by a non-linear regression analysis of NMR titration data,[25] and by using the data processing program HypNMR.[31] The results were coincident within the experimental uncertainty, and are presented in Table 2. As is evident from Table 2,

Table 2
Association constants ($K_{\mathbf{1}\cdot\mathbf{G}}$) of 1:1 adducts of *p*-sulfonatocalix[7]arene **1** with different guests

Guest	log $K_{\mathbf{1}\cdot\mathbf{G}}\pm3\sigma$	
	HypNMR	Non-linear regression
Diquat	4.6±0.2	4.57±0.05
Paraquat	4.5±0.1	4.5±0.1
Chlormequat	4.09±0.09	4.08±0.08

the doubly charged guests Diquat **2** and Paraquat **3** show a slightly higher affinity for *p*-sulfonatocalix[7]arene (**1**) than singly charged Chlormequat 4 suggesting that the binding of these charged guests is influenced by the strength of electrostatic interactions between sulfonato and ammonium groups.

2.3. Spectrofluorimetric determination of Diquat, Paraquat, and Chlormequat

Considering the good affinity of **1** toward **2**, **3**, and **4**, we decided to investigate the possibility to use **1** to detect their presence in the environment. To this purpose, a spectrofluorimetric method was used, which was based on the use of Acridine Orange (**5**), as

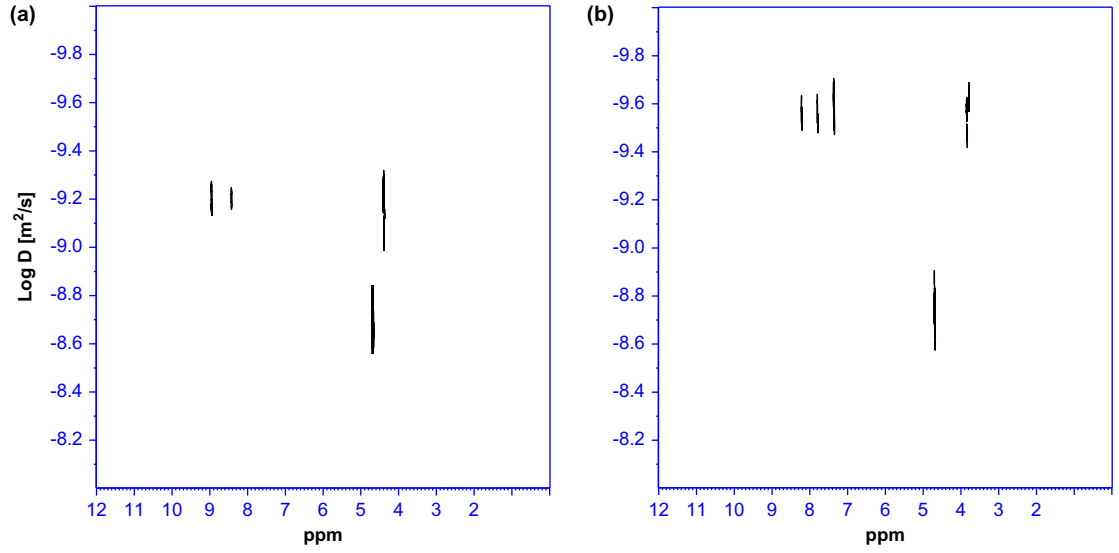

Figure 9. 2D-DOSY spectra recorded in 0.1 M deuterated phosphate buffer, pD 7.3 at 300 K with: (a) Paraquat **3** and (b) mixture of *p*-sulfonatocalix[7]arene **1** and **3** in a 1:1 ratio.

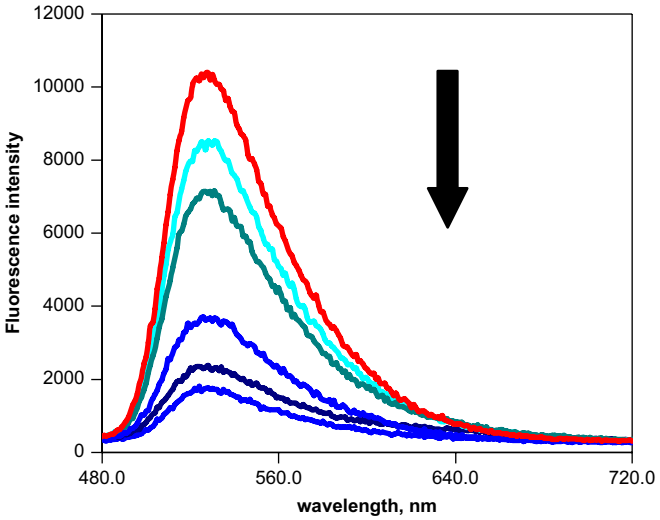

Figure 10. Fluorescence spectra of Acridine Orange **5** ($1.0\cdot10^{-6}$ M) in the presence and absence of *p*-sulfonatocalix[7]arene **1** (10^{-6} M): 0.0; 0.025; 0.050; 0.10; 1.0; 10.0, in aqueous solution at pH=7; fluorescence decrease by addition of **1** to **5**.

a chemical indicator of the binding of **2** or **3** to **1**. Actually, the detectable emission of **5** at 525 nm is suppressed in the presence of **1**, owing to the formation of adduct, according to reaction 6 the equilibrium constant of which is $K_{\mathbf{1}\cdot\mathbf{5}}$.

$$\mathbf{1}+\mathbf{5}\rightleftarrows\mathbf{1}\cdot\mathbf{5} \tag{6}$$

The decrease in fluorescence intensity of Acridine Orange upon the addition of calixarenesulfonate was mainly attributed to the inclusion complexation.[32] The decrease in fluorescence intensity by addition of **1** to **5**, as evidenced in Figure 10, allowed to determine, through the Benesi–Hildebrand method,[33] the association constant of **1**·**5**. Assuming a 1:1 stoichiometry,

$$\mathbf{H}+\mathbf{G}\rightleftarrows\mathbf{H}\cdot\mathbf{G} \tag{7}$$

the inclusion complexation of the Acridine Orange (**5**) with the *p*-sulfonatocalix[7]arene **1** is expressed by Eq. 7 and the complex stability constant (K_s) is given by Eq. 8.

$$K_{\text{ass}}=\frac{[\mathbf{HG}]}{[\mathbf{H}][\mathbf{G}]} \tag{8}$$

It is well-known that the fluorescence intensity is proportional to the concentration of the fluorophore in dilute solution,[34] therefore

$$\Delta F=\Delta\varepsilon\cdot[\mathbf{HG}] \tag{9}$$

where ΔF and $\Delta\varepsilon$ denote the changes in the fluorescence intensity and molar fluorescence intensity of the Acridine Orange upon complexation with calixarenesulfonate.

Under the conditions employed, the initial concentration of the guest is much larger than that of the host, i.e., $[\mathbf{G}_0]\gg[\mathbf{H}_0]$. Therefore, the combination of Eqs. 8 and 9 leads to the extended Benesi–Hildebrand equation (Eq. 10),[34] which was used to calculate the complex stability constants from the slope and intercept of $[\mathbf{H}_0][\mathbf{G}_0]/\Delta F$ versus $[\mathbf{H}_0]$ plots.

$$\frac{[\mathbf{H}_0][\mathbf{G}_0]}{\Delta F}=\frac{1}{K_{\text{ass}}\Delta\varepsilon}+\frac{[\mathbf{H}_0]}{\Delta\varepsilon} \tag{10}$$

A typical plot of this function for the complexation of Acridine Orange (**5**) with the *p*-sulfonatocalix[7]arene **1** to 25 °C in aqueous solution is illustrated in Figure 11, where the $[\mathbf{H}_0][\mathbf{G}_0]/\Delta F$ values are plotted against the $[\mathbf{H}_0]$ values, affording an excellent linear relationship according to the Benesi–Hildebrand Eq. 10. From the slope and intercept of the straight line the values of $K_{\text{ass}}=(19{,}130\pm50)\ \text{M}^{-1}$ and $\Delta\varepsilon=8.6\ \text{M}^{-1}$ have been calculated. The

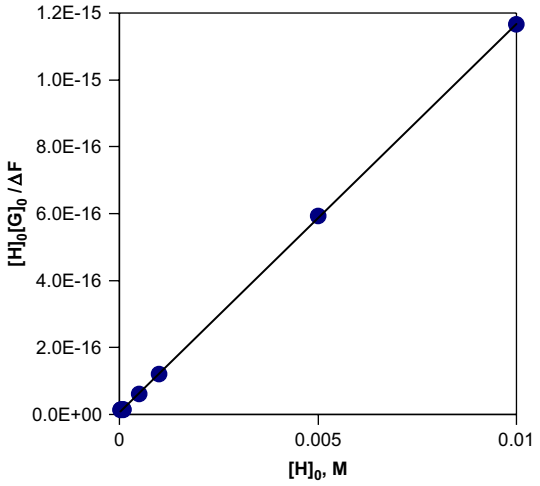

Figure 11. Typical plot of $[\mathbf{H}_0][\mathbf{G}_0]/\Delta F$ versus $[\mathbf{H}_0]$ for the complexation of Acridine Orange (**5**) with *p*-sulfonatocalix[7]arene **1** at 25 °C in aqueous solution.

value obtained, valid at 25 °C and at zero ionic strength, was $\log K_{\mathbf{1}\cdot\mathbf{5}}=4.283\pm0.007$ (uncertainty is 3σ) to be compared with the ones reported in Table 2. Accordingly to Table 2, it appears evident that only the detection of **2** or **3** is possible as far as the displacement reaction 11 proceeds.

$$\mathbf{1}\cdot\mathbf{5}+\mathbf{G}\rightleftarrows\mathbf{1}\cdot\mathbf{G}+\mathbf{5} \tag{11}$$

In reaction 11, **G** is **2** or **3**, and **1**·**G** represents the complexes of **2** or **3** with **1**. None of the species appearing in reaction 5 had a significant UV–vis emission except **5**, whose fluorescence emission at 525 nm increased as far as it was displaced from **1**·**5** by **G**. In Figure 12, the fluorescence spectrum of **1**·**5** solutions in the presence of increasing amounts of **2** is presented. The fluorescence emission intensity at 525 nm increases linearly with the concentration of **2**, added to **1**·**5**, up to 40 μM.

Therefore, this approach could be used as a fluorometric method for the detection of organic quaternary ammonium ion **2** of environmental relevance in aqueous solution. Similar behavior was observed for **3** (see Figs. S9 and S10 in Supplementary data).

In order to check the analytical usefulness of this method for the determination of Paraquat and Diquat, we have analyzed various solutions at various concentration of organic quaternary ammonium ion. The assessed detection limit is not inferior to

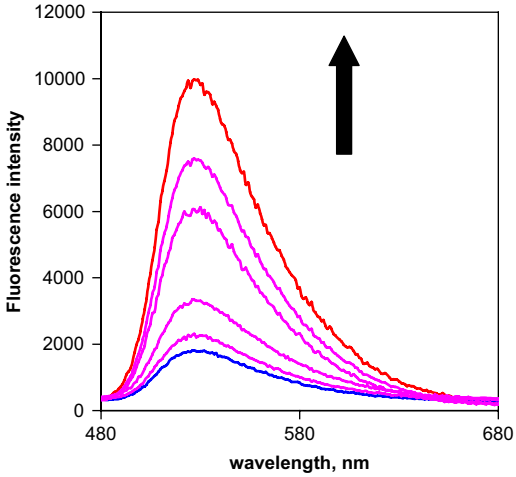

Figure 12. Fluorescence spectra of Acridine Orange **5** ($1.0\cdot10^{-6}$ M) in the presence of *p*-sulfonatocalix[7]arene **1** ($1.0\cdot10^{-5}$ M), in aqueous solution at pH=7; fluorescence intensity increase by addition of **2** (μM): 0.0; 1.0; 10.0; 20.0; 30.0; 40.0, to **1**·**5**.

0.1 mg/dm^3. This value can be compared to the health advisory levels usually established for Paraquat of 0.1 mg/L (children short-term exposure) and 0.2 mg/L (adult intermediate-term exposure) (EPA 734-12-92-001), and to its maximum contaminant limit (MCL) in drinking water of 3 μg/L.

3. Conclusion

In summary, the water-soluble *p*-sulfonatocalix[7]arene derivative **1** was synthesized through standard procedures. In accordance with the results of Harada and Shinkai for *p-tert*-butylcalix[7]arene, Monte Carlo conformational searches indicate the *double-cone pinched* conformation as the lowest energy conformation for *p*-sulfonatocalix[7]arene. The acid–base properties of **1** were investigated by means of potentiometric titration, obtaining pK_a values (pK_{a1}=3.19; pK_{a2}=5.40, pK_{a3}=9.41, pK_{a4}=12.0) in agreement with those reported for analogous *p*-sulfonatocalix[*n*]arenes (*n*=5 and 6). Analogously to these macrocycles, **1** also possesses two readily ionizable protons, and thereby at pH=7 it exists as the [*p*-sulfonatocalix[7]arene]$^{9-}$ anion. The binding ability of **1** toward organic quaternary ammonium cations such as Diquat (**2**), Paraquat (**3**), and Chlormequat (**4**) was investigated by means of ^{1}H NMR titrations in D_2O at pD=7.3. The more highly charged guests Diquat **2** and Paraquat **3** showed a slightly higher affinity for *p*-sulfonatocalix[7]arene than Chlormequat **4**, indicating that the complexation of these charged guests is driven by electrostatic interactions between sulfonato and ammonium groups. NMR and molecular mechanics studies indicate that both Diquat **2** and Paraquat **3** are sandwiched between the aromatic walls of the calixarene cavity with positive nitrogen atoms close to sulfonato groups to maximize electrostatic interactions, whereas Chlormequat 4 leads the ammonium methyl protons into the calixarene cavity to give C–H$\cdots\pi$ interactions.

4. Experimental

4.1. General

Reagents, characterization techniques, 1D and 2D NMR spectra, and energy-minimized structures of the complexes are described in the Supplementary data.

4.2. Synthesis

p-H-Calix[7]arene[19] (4.67 g, 6.3 mmol) was mixed with 30 mL of H_2SO_4 and the solution was heated at 80 °C for 3 h. After cooling, the precipitate was recovered by filtration. The precipitate was dissolved in water, and the solution was added of $Ba(OH)_2$ until pH=4–5. Precipitated $BaSO_4$ was removed by centrifugation, and then Na_2CO_3 (0.5 M aqueous solution) was added to the filtrate until pH=8–9. The solution was concentrated and treated with active charcoal. The filtrate was concentrated in vacuo, and ethanol was added to the remaining solution to give nonasodium salt of calix[7]arene-*p*-heptasulfonate **1** (yield 71%) as a white precipitate. ^{1}H NMR (400 MHz, D_2O, 298 K): δ 4.01 (s, $ArCH_2Ar$, 14H), 7.51 (s, ArH, 14H); ^{13}C NMR (100 MHz, D_2O, 298 K): δ 31.9 (t, $ArCH_2Ar$), 126.9 (d, $C_{Ar}H$), 129.6 (s, C_{Ar}), 132.8 (s, C_{Ar}), 157.3 (s, C_{Ar}); mp: 300 °C (decomp.); Anal. Calcd for $C_{49}H_{33}O_{28}S_7Na_9\cdot 8H_2O$: C, 35.77%; H, 3.00%; Na, 12.57%. Found: C, 35.68%; H, 3.08; Na, 12.65%.

4.3. Binding studies

^{1}H NMR titrations were performed at 298 K in D_2O. Chemical shifts were externally referenced to DSS (3-trimethylsilyl 1-propanesulfonic acid, sodium salt). All experiments were performed in deuterated phosphate buffer (0.1 M) with a pD value of 7.3. The guest concentration was kept constant while the host concentration was varied, examples: (Diquat) [**2**]=1.40 mM, [**1**]=0.16–3.40 mM; (Paraquat) [**3**]=1.80 mM, [**1**]=0.30–3.04 mM; (Clormequat) [**4**]=1.80 mM, [**1**]=0.13–3.59 mM. In all cases, the signals of the guest were followed and the data were analyzed by a non-linear regression analysis,[25] and by using the data processing program HypNMR.[31]

Supplementary data

Supplementary data associated with this article can be found in the online version, at doi:10.1016/j.tet.2008.03.017.

References and notes

1. (a) Lehn, J. M. *Supramolecular chemistry: Concepts and Perspectives*; VCH: Weinheim, 1995; (b) Steed, J. W.; Atwood, J. L. *Supramolecular Chemistry*; John Wiley & Sons: Chichester, UK, 2000.
2. (a) *Chemosensors for Ion and Molecule Recognition*; Czarnik, A. W., Desvergne, J.-P., Eds.; Kluwer: Dordrecht, 1997; For general reviews on mass sensors, see: (b) Van Veggel, F. C. J. M. *Comprehensive Supramolecular Chemistry*; Pergamon: Oxford, 1996; Vol. 10, pp 171–185; For general reviews on electrochemical sensors, see: (c) Brzózka, Z. *Comprehensive Supramolecular Chemistry*; Pergamon: Oxford, 1996; Vol. 10, pp 187–212; (d) Beer, P. D.; Gale, P. A. *Angew. Chem., Int. Ed.* **2001**, *40*, 486–516; (e) Tucker, J. H. R. *Encyclopedia of Supramolecular Chemistry*; Atwood, J. L., Steed, J. W., Eds.; Dekker: New York, NY, 2002; pp 505–519 and references therein; For general reviews on fluorescent sensors, see: (f) Bryan, A. J.; de Silva, A. P.; de Silva, S. A.; Rupasinghe, R. A. D. D.; Sandanayake, K. R. A. S. *Biosensors* **1989**, *4*, 169–179; (g) de Silva, A. P.; Gunaratne, H. Q. N.; Gunnlaugsson, T.; Huxley, A. J. M.; McCoy, C. P.; Rademacher, J. T.; Rice, T. E. *Chem. Rev.* **1997**, *97*, 1515–1566; (h) de Silva, A. P.; McClean, G. D.; Moody, T. S. *Encyclopedia of Supramolecular Chemistry*; Atwood, J. L., Steed, J. W., Eds.; Dekker: New York, NY, 2002; pp 572–578 and references therein; For general reviews on photochemical sensors, see: (i) Fabbrizzi, L. *Encyclopedia of Supramolecular Chemistry*; Atwood, J. L., Steed, J. W., Eds.; Dekker: New York, NY, 2002; pp 1053–1059 and references therein.
3. Lamb, J. D.; Smith, R. G. *Comprehensive Supramolecular Chemistry*; Pergamon: Oxford, 1996; Vol. 10, pp 79–112.
4. For a review on separation processes based on solid supported hosts, see: (a) Izatt, R. M.; Bradshaw, J. S.; Bruening, R. L.; Tarbet, B. J.; Bruening, M. L. *Comprehensive Supramolecular Chemistry*; Pergamon: Oxford, 1996; Vol. 10; pp 1–11; For recent examples of membranes containing calixarene hosts, see: (b) Kumar, P. L.; Saxena, C.; Dubey, V. *J. Membr. Sci.* **2003**, *227*, 173–182; (c) Uragami, T.; Meotoiwa, T.; Miyata, T. *Macromolecules* **2003**, *36*, 2041–2048; (d) Toutianoush, A.; El-Hashani, A.; Schnepf, J.; Tieke, B. *Appl. Surf. Sci.* **2005**, *246*, 430–436.
5. For general reviews on calixarenes, see: (a) Böhmer, V. *Angew. Chem., Int. Ed. Engl.* **1995**, *34*, 713–745; (b) Gutsche, C. D. *Calixarenes Revisited*; Royal Society of Chemistry: Cambridge, 1998; (c) *Calixarenes 2001*; Asfari, Z., Böhmer, V., Harrowfield, J., Vicens, J., Eds.; Kluwer: Dordrecht, 2001; (d) Böhmer, V. *The Chemistry of Phenols*; Rappoport, Z., Ed.; Wiley: Chichester, UK, 2003, Chapter 19; (e) *Calixarenes in the Nanoworld*; Vicens, J., Harrowfield, J., Eds.; Springer: Dordrecht, 2006.
6. (a) Shinkai, S.; Mori, S.; Tsubaki, T.; Sone, T.; Manabe, O. *Tetrahedron Lett.* **1984**, *25*, 5315–5318; (b) Shinkai, S.; Mori, S.; Koreishi, K.; Tsubaki, T.; Manabe, O. *J. Am. Chem. Soc.* **1986**, *108*, 2409–2416; (c) Shinkai, S.; Araki, K.; Tsubaki, T.; Arimura, T.; Manabe, O. *J. Chem. Soc., Perkin Trans. 1* **1987**, 2297–2299; (d) Shinkai, S.; Mori, S.; Araki, T.; Manabe, O. *Bull. Chem. Soc. Jpn.* **1987**, *60*, 3679–3685; (e) Arimura, T.; Edamitsu, S.; Shinkai, S.; Manabe, O.; Muramatsu, T.; Tashiro, M. *Chem. Lett.* **1987**, 2269–2272; (f) Coleman, A. W.; Bott, S. G.; Morley, S. D.; Means, C. M.; Robinson, K. D.; Zhang, H.; Atwood, J. L. *Angew. Chem., Int. Ed. Engl.* **1988**, *27*, 1412–1413; (g) Shinkai, S.; Araki, K.; Matsuda, T.; Nishiyama, N.; Ikeda, H.; Takasu, I.; Iwamoto, M. *J. Am. Chem. Soc.* **1990**, *112*, 9053–9058; (h) Steed, J. W.; Johnson, C. P.; Barnes, C. L.; Juneja, R. K.; Atwood, J. L.; Reilly, S.; Hollis, R. L.; Smith, P. H.; Clark, D. L. *J. Am. Chem. Soc.* **1995**, *117*, 11426–11433; (i) Casnati, A.; Sciotto, D.; Arena, G. *Calixarenes 2001*; Asfari, Z., Böhmer, V., Harrowfield, J., Vicens, J., Eds.; Kluwer: Dordrecht, 2001; pp 440–456, Chapter 24 and references therein.
7. (a) Douteau-Guevel, N.; Coleman, A. W.; Morel, J.-P.; Morel-Desrosiers, N. *J. Phys. Org. Chem.* **1998**, *11*, 693–696; (b) Douteau-Guevel, N.; Coleman, A. W.; Morel, J.-P.; Morel-Desrosiers, N. *J. Chem. Soc., Perkin Trans. 2* **1999**, 629–634; (c) Arena, G.; Contino, A.; Gulino, F. G.; Magrì, A.; Sansone, F.; Sciotto, D.; Ungaro, R. *Tetrahedron Lett.* **1999**, *40*, 1597–1600; (d) Kalchenko, O. I.; Perret, F.; Morel-Desrosiers, N.; Coleman, A. W. *J. Chem. Soc., Perkin Trans. 2* **2001**, 258–263; (e) Da Silva, E.; Coleman, A. W. *Tetrahedron* **2003**, *59*, 7357–7364; (f) Arena, G.; Casnati, A.; Contino, A.; Magrì, A.; Sansone, F.; Sciotto, D.; Ungaro, R. *Org. Biomol. Chem.* **2006**, *4*, 243–249; (g) Nichols, P. J.; Makha, M.; Raston, C. L. *Cryst. Growth Des.* **2006**, *6*, 1161–1167.
8. Douteau-Guevel, N.; Perret, F.; Coleman, A. W.; Morel, J.-P.; Morel-Desrosiers, N. *J. Chem. Soc., Perkin Trans. 2* **2002**, 524–532.
9. (a) Specht, A.; Ziarelli, F.; Bernard, P.; Goeldner, M.; Peng, L. *Helv. Chim. Acta* **2005**, *88*, 2641–2653; (b) Liu, Y.; Yang, E.-C.; Chen, Y.; Guo, D.-S.; Ding, F. *Eur.*

J. Org. Chem. **2005**, 4581–4588; (c) Liu, Y.; Guo, D.-S.; Yang, E.-C.; Zhang, H.-Y.; Zhao, Y.-L. *Eur. J. Org. Chem.* **2005**, 162–170; (d) Smith, C. B.; Makha, M.; Raston, C. L.; Sobolev, A. N. *New J. Chem.* **2007**, *31*, 535–542.
10. Bakirci, H.; Koner, A. L.; Nau, W. M. *J. Org. Chem.* **2005**, *70*, 9960–9966.
11. (a) Millership, J. S. *J. Inclusion. Phenom. Macrocycl. Chem.* **2001**, *39*, 327–331; (b) Da Silva, E.; Valmalle, C.; Becchi, M.; Cuilleron, C.-Y.; Coleman, A. W. *J. Inclusion. Phenom. Macrocycl. Chem.* **2003**, *46*, 65–69.
12. (a) Lehn, J. M.; Meric, R.; Vigneron, J.-P.; Cesario, M.; Guilhem, J.; Pascard, C.; Asfari, Z.; Vicens, J. *Supramol. Chem.* **1995**, *5*, 97–103; (b) Jin, T. *J. Inclusion. Phenom. Macrocycl. Chem.* **2003**, *45*, 195–201.
13. (a) Stödeman, M.; Dhar, N. *Thermochim. Acta* **1998**, *320*, 33–88; (b) Stödeman, M.; Dhar, N. *J. Chem. Soc., Faraday Trans.* **1998**, *94*, 899–903; (c) Arena, G.; Casnati, A.; Contino, A.; Lombardo, G. G.; Sciotto, D.; Ungaro, R. *Chem.—Eur. J.* **1999**, *5*, 738–744; (d) Arena, G.; Casnati, A.; Contino, A.; Gulino, F. G.; Sciotto, D.; Ungaro, R. *J. Chem. Soc., Perkin Trans. 2* **2000**, 419–423; (e) Bonal, C.; Israëli, Y.; Morel, J.-P.; Morel-Desrosiers, N. *J. Chem. Soc., Perkin Trans. 2* **2001**, 1075–1078; (f) Mendes, A.; Bonal, C.; Morel-Desrosiers, N.; Morel, J.-P.; Malfreyt, P. *J. Phys. Chem. B* **2002**, *106*, 4516–4524.
14. (a) Liu, Y.; Guo, D.-S.; Zhang, H.-Y.; Ma, Y.-H.; Yang, E.-C. *J. Phys. Chem. B* **2006**, *110*, 3428–3434; (b) Liu, Y.; Guo, D.-S.; Zhang, H.-Y.; Ding, F.; Chen, K.; Song, H.-B. *Chem.—Eur. J.* **2007**, *13*, 466–472; (c) Guo, D.-S.; Wang, L.-H.; Liu, Y. *J. Org. Chem.* **2007**, *72*, 775–778.
15. For a review on the chemistry of calix[7]arenes, see: Martino, M.; Neri, P. *Mini-Rev. Org. Chem.* **2004**, *1*, 219–231 and references cited therein.
16. Andreetti, G. D.; Ugozzoli, F.; Nakamoto, Y.; Ishida, S. I. *J. Inclusion. Phenom. Macrocycl. Chem.* **1991**, *10*, 241–253.
17. Harada, T.; Shinkai, S. *J. Chem. Soc., Perkin Trans. 2* **1995**, 2231–2242.
18. Stewart, D. R.; Gutsche, C. D. *J. Am. Chem. Soc.* **1999**, *121*, 4136–4146.
19. (a) Markowitz, M. A.; Janout, V.; Castner, D. G.; Regen, S. L. *J. Am. Chem. Soc.* **1989**, *111*, 8192–8200; (b) Benjamin, Y.; Bassus, J.; Lamartine, R. *An. Quim. Int. Ed.* **1998**, *94*, 65–66.
20. *MacroModel, version 9.0*; Schrödinger, LLC: New York, NY, 2005; Mohamadi, F.; Richards, N. G.; Guida, W. C.; Liskamp, R.; Lipton, M.; Caufield, C.; Chang, G.; Hendrickson, T.; Still, W. C. *J. Comput. Chem.* **1990**, *11*, 440–467.
21. For the pleated-loop/cone conformation reported for *p*-ethylcalix[7]arene, see: (a) Perrin, M.; Lecocq, S.; Asfari, Z. *C. R. Acad. Sci. Ser. 2* **1990**, *310*, 515–520; For an X-ray structure of *p-tert*-butylcalix[7]arene/UO_2 complex, in which the calix[7]arene skeleton adopts a conformation very similar to the double-cone pinched, see: (b) Thuery, P.; Nierlich, M.; Ogden, M. I.; Harrowfield, J. M. *Supramol. Chem.* **1998**, *9*, 297–303; For the X-ray structure of bis(*p*-benzylcalix[7]arene)/hexauranyl complex, see: (c) Thuery, P.; Nierlich, M.; Souley, B.; Asfari, Z.; Vicens, J. *J. Chem. Soc., Dalton Trans.* **1999**, 2589–2594; For the X-ray structure of *p*-benzylcalix[7]arene, see: (d) Atwood, J. L.; Hardie, M. J.; Raston, C. L.; Sandoval, C. A. *Org. Lett.* **1999**, *1*, 1523–1526; For the X-ray structure of *p-tert*-butylcalix[7]arene-heptacarboxylic acid, see: (e) Ludwing, R.; Lentz, D.; Nguyen, T. K. D. *Radiochim. Acta* **2000**, *88*, 335–343.
22. Biedermann, G. Ionic Media. In *On the Nature of Seawater*; Goldberg, E. D., Ed.; Dahlem Konferenzen: Berlin, 1975; p 339.
23. Gran, G. *Analyst* **1952**, *77*, 661–671.
24. For pK_a values of *p*-sulfonatocalix[*n*]arenes, see: *p*-sulfonatocalix[4]arene, (a) Arena, G.; Calì, R.; Lombardo, G. G.; Rizzarelli, E.; Sciotto, D.; Ungaro, R.; Casnati, A. *Supramol. Chem.* **1992**, *1*, 19–24; (b) Yoshida, I.; Yamamoto, N.; Sagara, F.; Ishii, D.; Ueno, K.; Shinkai, S. *Bull. Chem. Soc. Jpn.* **1992**, *65*, 1012–1015; *p*-Sulfonatocalix[5]arene, (c) see Ref. 6h; *p*-Sulfonatocalix[6]-arene and *p*-sulfonatocalix[8]arene, (d) Scharff, J. P.; Mahjoubi, M. *New J. Chem.* **1991**, *15*, 883–887; (e) Atwood, J. L.; Clark, D. L.; Juneja, R. K.; Orr, G. W.; Robinson, K. D.; Vincent, R. L. *J. Am. Chem. Soc.* **1992**, *114*, 7558–7559; (f) Arena, G.; Contino, A.; Lombardo, G. G.; Sciotto, D. *Thermochim. Acta* **1995**, *264*, 1–11.
25. (a) Connors, K. A. *Binding Constants*; John Wiley & Sons: Chichester, UK, 1987; (b) Wilcox, C. S. *Frontiers in Supramolecular Organic Chemistry and Photochemistry*; Schneider, H.-J., Dürr, H., Eds.; VCH: Weinheim, 1991; (c) Adrian, J. C.; Wilcox, C. S. *J. Am. Chem. Soc.* **1991**, *113*, 678–680; (d) Tsukube, H.; Furuta, H.; Odani, A.; Takeda, Y.; Kudo, Y.; Inoue, Y.; Liu, Y.; Sakamoto, H.; Kimura, K. *Comprehensive Supramolecular Chemistry*; Pergamon: Oxford, 1996; Vol. 10, pp 425–482; (e) Fielding, L. *Tetrahedron* **2000**, *56*, 6151–6170.
26. See Supplementary data for additional details.
27. (a) Kon, N.; Iki, N.; Miyano, S. *Org. Biomol. Chem.* **2003**, *1*, 751–755; (b) Arena, G.; Gentile, S.; Gulino, F. G.; Sciotto, D.; Sgarlata, C. *Tetrahedron Lett.* **2004**, *45*, 7091–7094.
28. (a) Gafni, A.; Cohen, Y. *J. Org. Chem.* **1997**, *62*, 120–125; (b) Frish, L.; Sansone, F.; Casnati, A.; Ungaro, R.; Cohen, Y. *J. Org. Chem.* **2000**, *65*, 5026–5030; (c) Frish, L.; Matthews, S. E.; Böhmer, V.; Cohen, Y. *J. Chem. Soc., Perkin Trans. 2* **1999**, 669–671; (d) Frish, L.; Vysotsky, M. O.; Matthews, S. E.; Böhmer, V.; Cohen, Y. *J. Chem. Soc., Perkin Trans. 2* **2002**, 88–93; (e) Avram, L.; Cohen, Y. *J. Org. Chem* **2002**, *67*, 2639–2644; (f) Cohen, Y.; Avram, L.; Frish, L. *Angew. Chem., Int. Ed.* **2005**, *44*, 520–554; (g) Gulino, F. G.; Lauceri, R.; Frish, L.; Evan-Salem, T.; Cohen, Y.; De Zorzi, R.; Geremia, S.; Di Costanzo, L.; Randaccio, L.; Sciotto, D.; Purrello, R. *Chem.—Eur. J.* **2006**, *12*, 2722–2729.
29. Dalgarno, S. J.; Hardie, M. J.; Makha, M.; Raston, C. L. *Chem.—Eur. J.* **2003**, *9*, 2834–2839.
30. Kestin, J.; Imaishi, N.; Nieuwoudt, J. C.; Sengers, J. V.; Nott, S. H. *Physica A* **1985**, 38–85.
31. Frassineti, C.; Ghelli, S.; Gans, P.; Sabatini, A.; Moruzzi, M. S.; Vacca, A. *Anal. Biochem.* **1995**, *231*, 374–382.
32. Liu, Y.; Han, B.-H.; Chen, Y.-T. *J. Org. Chem.* **2000**, *65*, 6227–6230.
33. Benesi, H. A.; Hildebrand, J. H. *J. Am. Chem. Soc.* **1949**, *71*, 2703–2707.
34. Rendell, D. *Fluorescence and Phosphorescence*; John Wiley & Sons: London, 1987; pp 91–93.